10.1098/rspa.2004.1300

THE ROYAL SOCIETY

Equation-free modelling of evolving diseases: coarse-grained computations with individual-based models

By Jaime Cisternas[1,2]†, C. William Gear[2,3], Simon Levin[4] and Ioannis G. Kevrekidis[1,2]

[1]*Program in Applied and Computational Mathematics and*
[2]*Department of Chemical Engineering,*
Princeton University, Princeton, NJ 08544,
USA (jcistern@princeton.edu; yannis@princeton.edu)
[3]*NEC Research Institute, Princeton, NJ 08540, USA*
[4]*Department of Ecology and Evolutionary Biology,*
Princeton University, Princeton, NJ 08544, USA

Received 2 October 2003; accepted 12 February 2004; published online 23 June 2004

We demonstrate how direct simulation of stochastic, individual-based models can be combined with continuum numerical-analysis techniques to study the dynamics of evolving diseases. Sidestepping the necessity of obtaining explicit population-level models, the approach analyses the (unavailable in closed form) 'coarse' macroscopic equations, estimating the necessary quantities through appropriately initialized short 'bursts' of individual-based dynamic simulation. We illustrate this approach by analysing a stochastic and discrete model for the evolution of disease agents caused by point mutations within individual hosts. Building up from classical susceptible–infected–recovered and susceptible–infected–recovered–susceptible models, our example uses a one-dimensional lattice for variant space, and assumes a finite number of individuals. Macroscopic computational tasks enabled through this approach include stationary-state computation, coarse projective integration, parametric continuation and stability analysis.

Keywords: influenza A drift; travelling wave; multiscale analysis; individual-based model; equation-free

1. Introduction

Classical models of disease dynamics rely on systems of differential equations that represent the numbers of individuals in various categories through continuous variables. This is especially problematic in examining the evolution of disease agents, since it ignores the stochastic and discrete nature of the dynamics of rare mutants. An equation-free multiscale computational approach may circumvent this problem, enabling individual-based stochastic simulations to analyse the macroscopic, *expected*

† Present address: Facultad de Ingeniería, Universidad de los Andes, San Carlos de Apoquindo 2200, Santiago, Chile.

epidemic dynamics directly. In this paper we will study the coarse-grained evolution of the empirical density function (EDF) of infected/recovered individuals over a lattice of virus strains. This evolution is driven by the genesis of new strains through mutation and an asymmetric cross-immunity kernel; these give rise to travelling-wave-like density dynamics whose dependence on parameters we study. The main computational tool is a two-level description: the lower level is a stochastic simulation of the discrete system, whose results are used to estimate features of the coarse model that are processed at the higher, continuum level. Assuming that continuum, population-level evolution equations for the coarse-grained epidemic dynamics exist (even though they are not available in closed form), we circumvent their explicit derivation using the so-called coarse time-stepper (Gear *et al.* 2002; Kevrekidis *et al.* 2003; Theodoropoulos *et al.* 2000).

Traditional continuum numerical-analysis codes typically operate by repeatedly calling—with the current state and parameters as input—a subroutine that contains the model, usually in the form of the time derivative of the population-level equations. The subroutine *evaluates* the model and returns the time derivative; possibly also partial derivatives with respect to the state variables (Jacobians), or with respect to parameters, are returned. The main code uses the results of these *function evaluations* to perform the computations underlying computational tasks such as numerical integration, steady-state computation (e.g. through Newton–Raphson iteration), stability, continuation and bifurcation computations. When explicit coarse-grained equations are available, the same type of repeated function evaluations underpin computational tasks such as optimization, controller design or the computation of coarse self-similar solutions.

In evolutionary epidemiology computations (as is often the case in contemporary modelling in the physical, life and social sciences) good system descriptions are often available at a fine-scale, stochastic, individual-based level. The closures required to translate the individual-based dynamics to macroscopic equations, amenable to systematic computer-aided analysis (such as bifurcation, stability, continuation and parametric analysis) are not available in closed form. Our equation-free multiscale computational framework replaces function evaluations (which we would perform if we had explicit macroscopic equations) with short bursts of appropriately initialized ensembles of simulations with the fine-scale, individual-based model. The results of these short simulations are used to *estimate* the same quantities (time derivatives, residuals, the action of Jacobians) that would be *evaluated* from a population-level model. The macroscopic tasks proceed in the same way, and with the same algorithms as before; the only difference is that function evaluation has been substituted by short bursts of microscopic/stochastic simulation and appropriate processing of the results (using established system-identification techniques).

This two-level (possibly multilevel) 'closure-on-demand' framework constitutes a bridge between simulation at a fine level (atomistic, individual based, stochastic) and exploration of emergent behaviour at a coarser level (macroscopic, averaged, expected). Remarkably, a large body of work on the so-called *matrix-free* large-scale scientific computation methods over the last twenty years fits directly in our multiscale framework; hence the 'equation-free' characterization. The approach, first proposed in Theodoropoulos *et al.* (2000) and discussed in detail in Kevrekidis *et al.* (2003), has been validated in a number of contexts: coarse kinetic Monte Carlo simulations of lattice gas models of surface reactions; coarse Brownian dynamics

for nematic liquid crystals; coarse molecular dynamics of peptide fragments; and coarse lattice Boltzmann simulations of multiphase flow, to name a few. A discussion of the approach, containing references to related approaches, such as the optimal predictors of Chorin and co-workers (Chorin *et al.* 1998, 2000), as well as the quasi-continuum method of Phillips, Ortiz and co-workers (Shenoy *et al.* 1999), can be found in Kevrekidis *et al.* (2003); for relations with accelerated molecular-dynamics techniques see Hummer & Kevrekidis (2003). This is our first attempt at using this approach in an epidemiological (and in particular in an evolutionary, mutation-based) context. Coarse integration schemes, in our illustrative example, will accelerate the direct simulation of the expected epidemic dynamics. Fixed-point algorithms will be used to converge on stationary drifting population 'pulse' shapes, their expected drift speeds, and their dependence on model parameters, including the overall population size.

To motivate our susceptible–infected–recovered–susceptible-type (SIRS-type) evolutionary illustrative example, it is interesting to draw some parallels with the special case of the evolution of the influenza virus. Influenza is one of the most familiar diseases humans face, having coexisted with us for perhaps four centuries. Despite this, and despite the fact that recovery from a particular strain of flu confers lifetime resistance, the disease remains a scourge, killing millions annually (Earn *et al.* 2002). The key reason lies in the evolutionary dynamics of the virus.

Study of the evolution of the influenza virus has been greatly enhanced in recent years by advances in molecular biology, and has helped elucidate the unusual phylogenetic patterns that emerge. In particular (Fitch *et al.* 2000), the evolutionary tree of the most common (H3N2) subtype of the influenza A virus has the form of a single major trunk, with limited variation about it. This makes it possible to study the evolution of the virus in terms of movement along a one-dimensional (1D) continuum, as presented by Lin *et al.* (2003).

In this work we want to study evolutionary epidemiological models without making the assumptions of an infinite population and a continuous space of variants. The total population is taken to consist of a finite number of individuals (of the order of 10^2–10^7), and the space of variants is a discrete 1D lattice. The apparent asymptotic behaviour of the stochastic model consists of effectively stationary shape-population 'pulses', drifting at an essentially constant rate over variant space. The paper is organized as follows. In § 2 our stochastic, individual-based model will be presented. Coarse computational methods are described in § 3, and the results of their application constitute § 4. We conclude with a brief discussion in § 5.

2. The stochastic model

Our SIRS-type illustrative model is partly based on certain features of influenza A virus evolution. Following an approach of Pease (1987), Andreasen *et al.* (1996) developed a continuum model for the evolution of a virus. In particular, they characterize individuals according to the last strain of the virus they experienced, since this is the best indicator of current susceptibility. For influenza A, recovery from (or vaccination against) a particular strain of the virus confers lifetime immunity not only to that strain, but also (at least partly) to the closely related strains that appear in subsequent years. Based on this they demonstrate that asymptotic travelling waves form in a continuum model and move with a characteristic speed through sequence

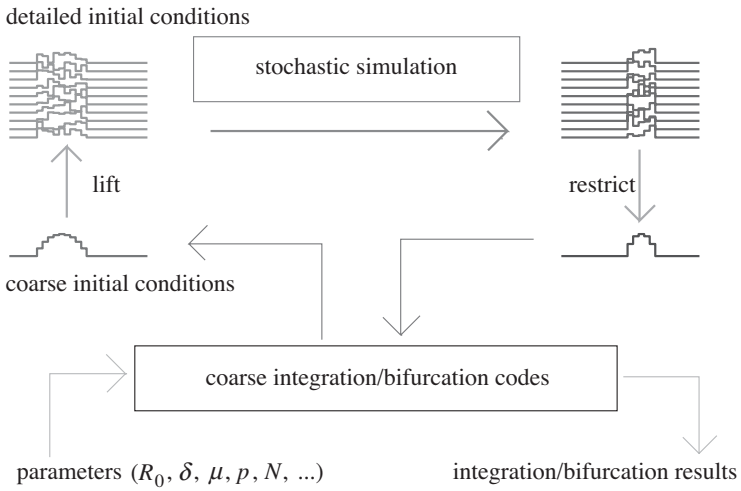

Figure 1. Schematic of the coarse time-stepper, employing a low-dimensional representation for the system statistics, lifting and restriction operators, and the individual-based, stochastic simulation code. Evaluating this time-stepper for appropriate sets of initial conditions helps estimate coarse-grained time derivatives, enables projective integration methods, as well as coarse fixed-point computation/continuation through matrix-free iterative algorithms.

space—a speed that can be compared with measured speeds of 'drift' evolution (the gradual change in the virus due to mutation and selection) (Lin *et al.* 2003). Earn *et al.* (2002), echoing Andreasen *et al.* (1996) and Lin *et al.* (2003), note that the continuum model is a gross approximation and that more accuracy would be possible with an individual-based model but at the cost of analytical tractability. Our coarse-grained approach aims at circumventing the analytical tractability issue; we solve the analytically unavailable equations by acting directly, through appropriately initialized and processed calls, to an individual-based simulator.

Our individual-based modelling builds upon classical SIRS-type models of an epidemic. For influenza A, the appropriate model would be SIR, since immunity in this case is permanent (Andreasen *et al.* 1996; Lin *et al.* 2003). Each individual in a population will be either susceptible ($\mathcal{S}$), infected ($\mathcal{I}$) or recovered ($\mathcal{R}$), meaning that he/she has not suffered the disease, is currently a carrier of the virus, or had the disease in the past and has immunity to a future infection. Other details like age, gender or time of residence in each category are not considered here. No interaction structure is assumed, so we use the equivalent of random mixing.

Our model, based on a 1D lattice of virus strains, is a compartmental one. We designate a single compartment $\mathcal{S}$ for totally naive individuals and use the variable $S \stackrel{\text{def}}{=} [\mathcal{S}] \in \mathbb{Z}_0^+$ for the number of individuals in $\mathcal{S}$. Compartments $\mathcal{I}_i$ and $\mathcal{R}_i$ contain individuals who are infected or have recovered from the strain i, respectively. The numbers of individuals in each compartment are $I \stackrel{\text{def}}{=} [\mathcal{I}_i]$ and $R \stackrel{\text{def}}{=} [\mathcal{R}_i]$. Note that the presence of an individual in compartment $\mathcal{I}_i$ or $\mathcal{R}_i$ means that the last transition for that individual was into that compartment. All prior history for that individual is lost. Possible changes of state (transition between compartments) are infections, recoveries, losses of immunity, births and deaths; the latter are not due to the dis-

Table 1. *Allowed transitions between different compartments and their corresponding Poisson-process expectations per individual (PPEPI)*

(In the birth process $\mathcal{X}$ implies any $\mathcal{S}$, $\mathcal{I}_i$ or $\mathcal{R}_i$ individual; the newborn individual is taken to be susceptible. A transition to $\emptyset$ means that an individual leaves the system (dies). For influenza A, immunity to a particular strain is lifelong so $\gamma = 0$. Subscripts refer to particular strains. $K_{i,j}$ is the relative susceptibility of an $\mathcal{R}_j$ individual to infection with strain i.)

transition	from	to	PPEPI
infections	$\mathcal{S}$	$\mathcal{I}_i$	$\beta I_i/N$
reinfections	$\mathcal{R}_j$	$\mathcal{I}_i$	$\beta K_{i,j} I_i/N$
recoveries	$\mathcal{I}_i$	$\mathcal{R}_i$	ν
births	$\mathcal{X}$	$\mathcal{X}+\mathcal{S}$	μ
deaths	$\mathcal{S}$	$\emptyset$	μ
	$\mathcal{I}_i$	$\emptyset$	μ
	$\mathcal{R}_i$	$\emptyset$	μ
losses of immunity	$\mathcal{R}_i$	$\mathcal{S}$	γ
mutations	$\mathcal{I}_i$	$\mathcal{I}_{i-1}$	$p/2$
	$\mathcal{I}_i$	$\mathcal{I}_{i+1}$	$p/2$

ease, and occur with equal probability for all compartments. The SIRS model also includes the loss of immunity after a certain period of time after the recovery (not the case for influenza A). As a result of errors in the replication of virions within the hosts, new variants of the virus are created. These new strains may be able to overcome the defences of individuals who had recovered from a previous epidemic.

Though all strains are assumed equal (in their dynamic rates), cross-immunity induces a hierarchy that explains a preferred direction in the time evolution of the epidemic outburst: the fact that an individual in $\mathcal{R}_i$ is immune to the disease carried by the $\mathcal{I}_j$ does not mean that individuals in $\mathcal{R}_j$ are immune to $\mathcal{I}_i$. In table 1 a summary of the transitions between compartments is presented, along with their Poisson-process expectations (all the processes are assumed to be Poisson). We define

$$I \stackrel{\text{def}}{=} \sum_i I_i, \quad R \stackrel{\text{def}}{=} \sum_i R_i \quad \text{and} \quad N \stackrel{\text{def}}{=} S + I + R.$$

The population size is not constant but for small μ the variation is small over finite-time computational horizons. While the simulation could proceed in an event-driven manner based on the Poisson processes, we have chosen to simulate in discrete time using a time-step small enough for the probability of an event in any transition category to be less than 0.01.

The Poisson-process expectations depend on the epidemiological parameters ν, μ, γ, β and p (in units of yr^{-1}). It is convenient to introduce the basic reproduction number (a non-dimensional quantity), $R_0 \stackrel{\text{def}}{=} \beta/(\nu+\mu)$, which expresses the number of individuals in a naive population that a carrier of the disease is expected to infect before recovery. Naturally, we need $R_0 > 1$ for long-lasting epidemics. We illustrate the method first for a hypothetical SIRS disease, with parameters: $\nu = 10\,\mathrm{yr}^{-1}$, $\mu = 1/60\,\mathrm{yr}^{-1}$, $\gamma = 1.5\,\mathrm{yr}^{-1}$, $p = 1.2\,\mathrm{yr}^{-1}$ and $R_0 = 10$. The value for the mutation rate was chosen somewhat high so that relatively smooth travelling pulses would arise at moderate population sizes. The random number generator used for the simulations

was a minimal standard generator (see Press *et al.* 1992). We used the generator of binomial deviates found in the same reference.

(*a*) *Single strain*

The behaviour of the basic SIR ($\gamma = 0$) and SIRS ($\gamma > 0$) model, assuming no mutation or reinfections at the fluctuation-free limit ($N \to \infty$), can be written in the form of three ordinary differential equations for the quantities S/N, I/N and $R/N \in [0, 1]$ (see, for example, Nåsell 1999). These equations have up to two fixed points, the disease-free state (extinction of the disease)

$$\frac{S}{N} = s^0 \stackrel{\text{def}}{=} 1, \qquad \frac{I}{N} = i^0 \stackrel{\text{def}}{=} 0, \qquad \frac{R}{N} = r^0 \stackrel{\text{def}}{=} 0,$$

and the epidemic equilibrium

$$\frac{S}{N} = s^* \stackrel{\text{def}}{=} \frac{1}{R_0},$$

$$\frac{I}{N} = i^* \stackrel{\text{def}}{=} \frac{(\mu+\gamma)}{(\nu+\mu+\gamma)}\left(1 - \frac{1}{R_0}\right),$$

$$\frac{R}{N} = r^* \stackrel{\text{def}}{=} \frac{\nu}{\nu+\mu+\gamma}\left(1 - \frac{1}{R_0}\right).$$

No epidemic equilibrium exists for $R_0 < 1$: the disease-free state is a stable fixed point. If $R_0 > 1$, the epidemic equilibrium is the only stable fixed point.

In a finite population ($N < \infty$) model there is a finite probability of reaching the extinction of the population state, $S = I = R = 0$, at any given time; this state is absorbing. There is also an absorbing *manifold* of disease-free states $I = 0$, reached after the recovery or death of the last infected individual. These two states play a vital role in determining the truly *long-term* expected behaviour of the discrete system; nevertheless, we will work in parameter regimes and with population sizes for which *over the time of our simulation/observation* the probability of such extinctions is negligibly small. While no direct equivalent to the deterministic epidemic equilibrium exists in this case, most initial conditions will first approach a region where $S/N \approx s^*$, $I/N \approx i^*$, $R/N \approx r^*$, spend some time there (proportional to N), then eventually decay to the disease-free manifold and ultimately get absorbed by the extinction state. Our observations can therefore be thought of as 'medium-time' (as opposed to truly long-time) expected behaviour. When the population size becomes smaller, and the probability of extinction over a finite observation horizon grows, models based on the dynamics of rare events become more appropriate than the ones we use here. See Nåsell (1999, 2002) for very conservative estimates of the extinction times for the disease. In the absence of mutations, all epidemics are therefore short-lived.

(*b*) *Multiple strains*

In the presence of mutations and reinfections, a carrier of a mutant virus in a new class will start to infect naive individuals, along with some individuals who are not immune enough to resist the new variant. The survival of the disease hinges on its ability to generate new variants before most of the population becomes immune.

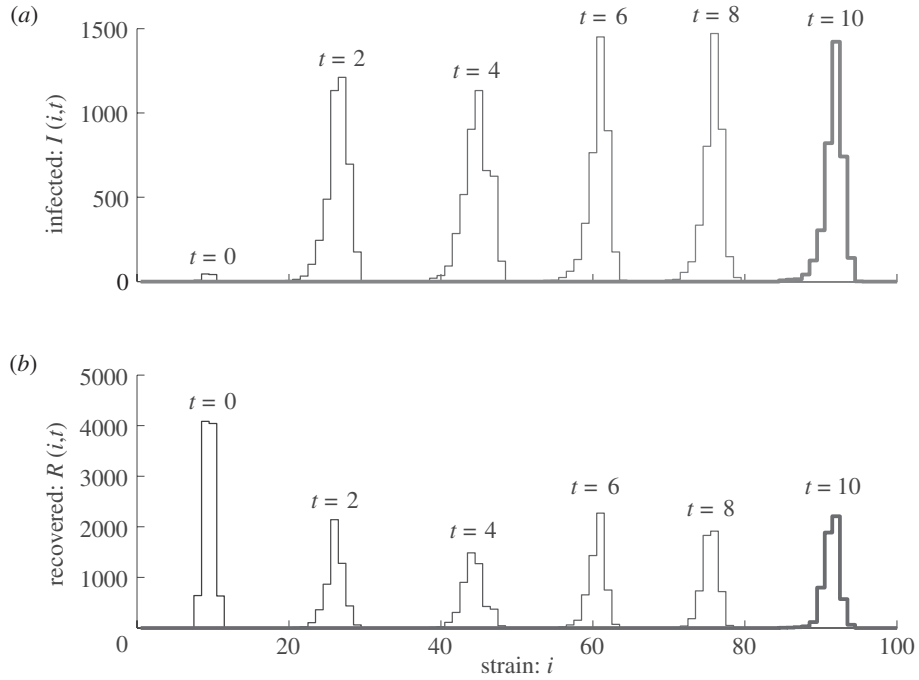

Figure 2. Evolution of the EDFs for a population of $N = 10\,000$ individuals over a year. Parameter values are $R_0 = 10$, $\nu = 60\ \mathrm{yr}^{-1}$, $\mu = 0.0167\ \mathrm{yr}^{-1}$, $\gamma = 1.5\ \mathrm{yr}^{-1}$ and $p = 1.2\ \mathrm{yr}^{-1}$. The EDF for (*a*) the infected and (*b*) the recovered populations.

Infectives are able to start epidemics in other variants, transmitting the disease to susceptible and recovered individuals with partial immunity, keeping high rates of infection for long periods of time.

To study the effect of mutations, we consider a 1D lattice $i \in \mathbb{Z}^+$ for the different strains and allow the reinfection of recovered individuals. We assume that, as for influenza, infection with the dominant strain in a given year provides partial protection against new mutant strains with an effectiveness (cross-reactivity or cross-immunity) that decays with time due to the continual evolution of the virus. Specifically, we use the model described in table 1 with the cross-immunity kernel from Lin *et al.* (2003):

$$K_{i,j} = K(i-j), \quad \text{with } K(\delta) = \begin{cases} 0 & \text{if } \delta < 0, \\ \dfrac{\delta}{(\delta + \delta_0)} & \text{otherwise.} \end{cases}$$

In this work we are using $\delta_0 = 5$. This kernel is clearly asymmetric and induces motion to the right (direction of increasing strain number), but respects discrete translational invariance.

Extensive simulations for this stochastic model typically reveal—depending on initial distribution, parameters and cross-immunity kernel—either a spreading out to zero or *apparent travelling pulses*.

Figure 2 shows snapshots of a realization of such a representative pulse. After a transient period, the sequence of infections, mutations, recoveries and reinfections

produces an effective drift in strain space. Both EDFs move in the same direction with similar widths but different amplitudes (the total numbers of susceptible and infected individuals are not the same). Estimates of the travelling speed in the doubly continuum (population and strain space) version of the model but for different parameters, namely $\gamma = 0$, are found in Lin *et al.* (2003), while Brunet & Derrida (1997, 1999) discuss the effect of finite population size in certain individual-based models with travelling-wave behaviour. We will study the *effective pulse speed* on N in our 'doubly discrete' model below (a feature reminiscent of other 'travelling pulses' in lattices (see Kessler *et al.* 1997; Ridgway *et al.* 1998)).

3. Methods

(*a*) *Coarse description: the inverse cumulative density function (ICDF)*

We seek continuum 'effective pulses' for our doubly discrete model. Representative simulations show that these 'pulses' have relatively localized support in strain space (for most of our simulations they are *ca.* 5–7 strains wide) and preserve their coarse shape (modulo random fluctuations) as they move. Additional fluctuations arise from the discreteness of the lattice, which only possesses *discrete* translational invariance. The study of effective-continuum equations for spatially discrete systems (lattices, such as this one) is the subject of extensive research; both analytical (Doering *et al.* 1987; Kevrekidis *et al.* 2002; Rosenau 1986, 1987, 1989, 1992) and equation-free approximations (Moeller *et al.* 2004) are possible. In what follows we will use averaging over several realizations of the microscopic simulation as well as spatial interpolation (filtering) to study the system dynamics in terms of *effective-continuum* observables. The effective pulses are slightly 'slanted' to the right, and this feature may get more pronounced if the mutation rate p is large or if the number of individuals N is small. The EDFs for the infected and recovered individuals are the number of individuals, $f(i)$, in each class, i. Low-dimensional approximations of the EDFs seem like natural macroscopic observation variables; we have chosen instead, and successfully used, low-dimensional representations of the ICDF, $g(p)$, also known as percentage point function (PPF). If the cumulative density function $G(i)$ is

$$G(i) = \sum_{j=0}^{i} f(j)/N,$$

then $g(p)$ is the inverse of $G(i)$.

Intuitively, $g(p)$ corresponds to the *location* (i.e. strain number) of individual Np after labelling all the individuals from left to right in strain space. When $f(i)$ appears as a localized pulse, $g(p)$ appears as the inverse of a sigmoid function (a monotonic function that transitions from zero to one over a finite, usually short, interval).

The ICDF is non-decreasing, and computations with its low-dimensional representation (e.g. coarse projective integration, or fixed-point estimation) should not destroy its monotonicity; sorting particle labels can restore monotonicity if necessary. For a finite number of individuals, $g(p)$ maps [0,1] into a bounded interval which moves as the wave travels; thus, the inverse CDF frees us from adjusting the CDF support as the simulation evolves. The drift towards the direction of increasing i is seen as an increase in its *average*, as its shape remains constant.

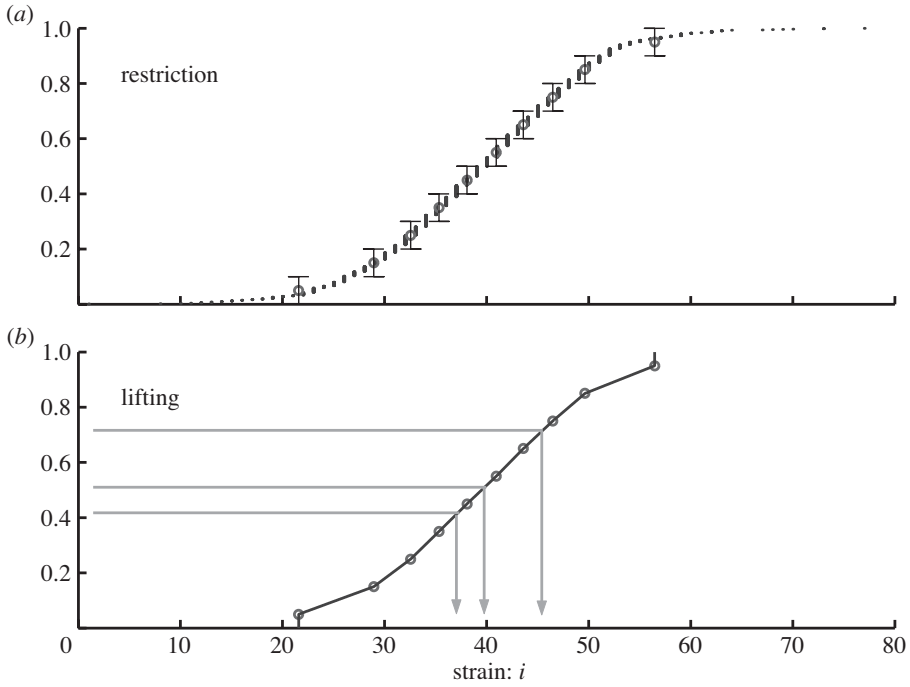

Figure 3. Restriction and lifting schemes. (*a*) Using the ICDF representation, we divide the [0,1] interval into 10 subintervals, separate the individuals accordingly, and compute the average strain of each subgroup, indicated with small circles. These averages are our low-dimensional representation of the density function. We use this reduction with infected and recovered individuals separately. (*b*) Using the averages on each subinterval, we can construct a density function using local linear interpolation and generating random numbers uniformly distributed in the interval [0,1] (vertical coordinate). The images of these points (in the horizontal coordinate) after being mapped with the piecewise linear function provide a distribution of individuals consistent with the coarse description of the density function.

Our low-dimensional representation of the coarse system state using the ICDF is made up of three components: the number of individuals in the classes $\mathcal{S}$, $\mathcal{I}$ and $\mathcal{R}$ expressed as ratios with respect to a *reference* number of individuals N_{ref}, the discrete ICDF for the $\mathcal{I}$ class $g_{\mathcal{I}}(x)$, and the discrete ICDF for the $\mathcal{R}$ class $g_{\mathcal{R}}(x)$. The vector describing the state of the whole population is then

$$\left\{ \frac{S}{N_{\mathrm{ref}}},\ \frac{I}{N_{\mathrm{ref}}},\ \frac{R}{N_{\mathrm{ref}}},\ g_{\mathcal{I}}(x_j)_{j=1,\ldots,M},\ g_{\mathcal{R}}(x_j)_{j=1,\ldots,M} \right\}.$$

Using 10 points to discretize the interval [0,1], our description for the coarse state involves 23 quantities. A graphical description of the scheme is presented in figure 3.

(*b*) *The coarse time-stepper*

We symbolize by $\Phi_\tau(\cdot)$ the following sequence of operations over a point in the low-dimensional representation y:

(i) lifting (initialization of a large number of realizations (S, I_i, R_i), each one consistent with y);

(ii) stochastic integration of each independent realization for a time τ;

(iii) restriction (estimation of the coarse state for each realization) and averaging over realizations (see figure 3).

Because the problem exhibits travelling behaviour, it is convenient to observe the simulation in a *co-moving frame*; in effect, this corresponds to a *shift* of the solution in (strain) space. Techniques for determining and effectively implementing this shift have been described in the literature (Chen & Goldenfeld 1995; Moeller *et al.* 2004; Rowley & Marsden 2000; Runborg *et al.* 2002); the amount of shift gives then an estimation of the travelling speed. Hence steps (i)–(iii) are followed by a fourth (iv) step: a shift in strain space, based on a so-called 'pinning condition'; the result of this shift is a new 'coarse point' $\Phi_\tau(y)$. Averaging over a large number of independent realizations reduces the fluctuations, even if each realization consists of a finite number of individuals. Techniques for variance reduction (Melchior & Oettinger 1995; Schoenmakers *et al.* 2002) can, in principle, also be used in evaluating the coarse time-stepper. The main assumption underlying our computational approach is that the coarse time-stepper *effectively commutes* with the integration (for time τ) of the unavailable macroscopic equations for the expected behaviour of the epidemic. Evaluating the coarse time-stepper through short bursts of appropriately initialized individual-based simulation allows us, as we will see below, to circumvent the derivation of explicit population-level evolution equations.

4. Results

We saw that, for a single realization, even with large populations the amplitudes of the pulses fluctuate around a mean shape/value, and the drift in strain space is often characterized by 'jerky' behaviour (figure 2). By averaging over many realizations starting with the same coarse initial condition we can drastically reduce the variance of these fluctuations, and approximate the evolution of an effective pulse. Figure 4 shows the evolution of a particular initial condition associated with a single initial strain; many copies (here 250) of this initial distribution are evolved in time with different random seeds. As the corresponding ICDFs evolve (by spreading and drifting) they all ultimately approach the same sigmoid translating profile. The (more or less) parallel lines are representative of the drift speed, and the (approximately one year long) transients are characteristic of the system's approach to its expected stationary drifting state.

(*a*) *Coarse projective integration*

Several realizations of the short-time stochastic evolution of an initial population with certain (coarse) characteristics can be used to *estimate* time derivatives of the expected evolution of these coarse characteristics. As discussed in detail in Kevrekidis *et al.* (2003) the duration of these stochastic simulation 'bursts' has to be long enough for the detailed features of the ICDFs to become functionals of (get slaved to) the coarse features. Indeed, the basic feature underlying a macroscopic model is a separation of time-scales between the low-order ('governing' or 'master') moments of a stochastically evolving distribution and the faster ('slave') higher moments. The singularly perturbed nature of the dynamics becomes manifest

as higher moments quickly become functionals of the lower-order ones, approaching a low-dimensional, attracting, invariant manifold in moments space. This manifold embodies, in effect, the closure giving rise to the lower-dimensional description. Variance reduction (e.g. through the number of realizations) as well as the duration of the stochastic simulation affects the quality of the time-derivative estimation. Using estimates of the time derivatives, we can implement explicit coarse integration. We call this approach 'projective forward integration' (Gear 2001; Gear & Kevrekidis 2003); more general extrapolation methods can also be used. This idea allows one to integrate the detailed problem only for a short period of time (healing time), estimate the slow evolution of coarse features and then project their future state.

The procedure is illustrated in figure 5. The lifting and restriction steps link the coarse and detailed descriptions of a state. The *projective* step is performed in the coarse description of the problem, followed by a new lifting step; the procedure is then repeated. Notice how a projective step may cause the solution to deviate from the 'slow manifold'; when the state lies on this manifold, higher-order moments of the evolving distribution can be expressed in terms of (have relaxed to being functionals of) a few lower-order, governing moments of the distribution. A short dynamic simulation *constrained* on the coarse projected state can be used as a preparation step, bringing the initialization closer to the slow manifold before letting it free; this is analogous to constrained molecular-dynamics algorithms like SHAKE (Carter *et al.* 1989; Ryckaert *et al.* 1977).

The method is especially successful in accelerating the simulation if a significant gap exists between the characteristic times of a few, slow modes (corresponding to the macroscopic, expected dynamics) and many fast ones (corresponding to the 'slaving' or 'healing' of the higher moments). Healing times here are of the order of 0.01 yr (depending on the quality of the macroscopic description and the number of independent copies), and characteristic times for the low-dimensional modes are of the order of 0.1 yr.

In figure 4*d* the results of a sequence of projective integrations are presented for comparison with the 'exact' integration (figure 4*a*). Thick lines correspond to detailed integrations, and thin lines to projections based on estimates of time-derivatives. As we can appreciate, the time horizon used for the detailed integrations ($\tau = 0.05$ yr) was long enough to allow healing, but small enough to capture the meaningful dynamics of the coarse variables, in particular the transients in the first 0.5 yr.

(*b*) *Coarse fixed-point computations*

For translationally invariant problems with travelling solutions, transforming to a co-travelling frame renders these solutions steady. This transformation can be performed dynamically without *a priori* knowledge of the right speed. Constantly shifting the solution back in (strain) space through a template-based so-called 'pinning condition' will turn a travelling solution into a stationary one (Rowley & Marsden 2000; Rowley *et al.* 2003); in effect, we are observing the computation in a co-travelling frame. In the absence of explicitly closed evolution equations this procedure can be implemented in discrete time (Runborg *et al.* 2002). Travelling pulses thus become fixed points of the (dynamically re-shifted) coarse time-stepper:

$$y - \Phi_\tau(y) = 0.$$

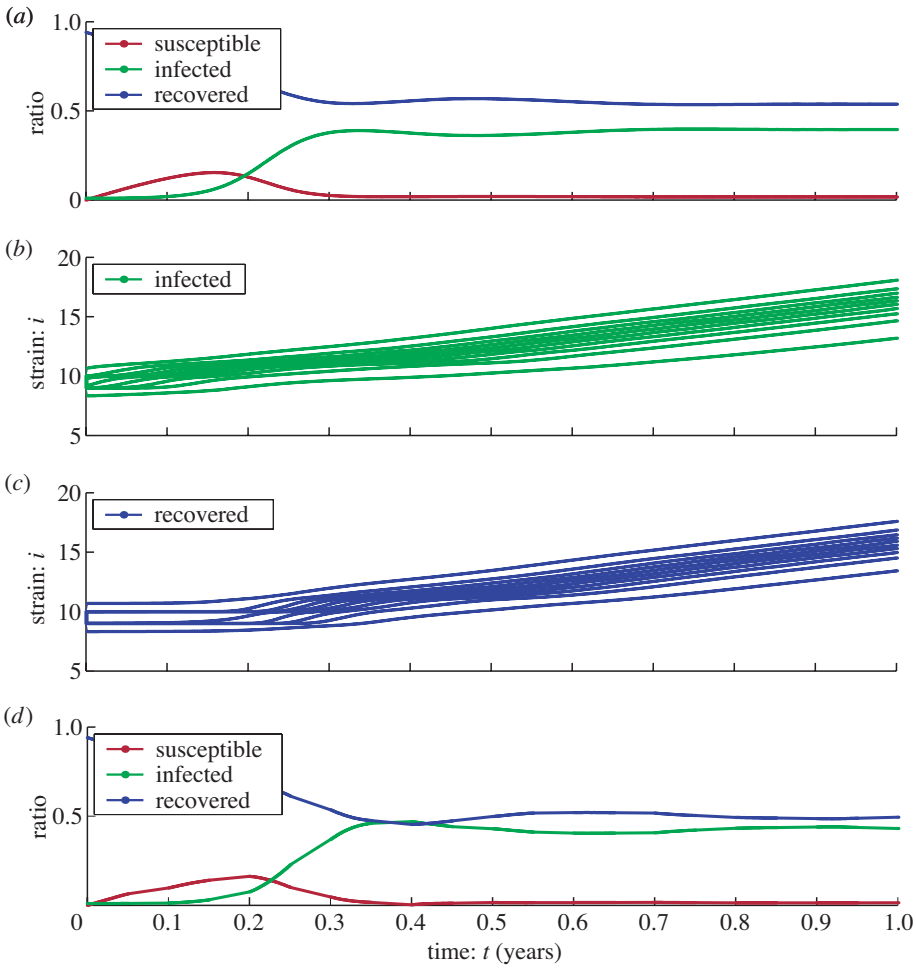

Figure 4. (*a*)–(*c*) Evolution of the average over 250 independent copies of the system, each one containing around 10 000 individuals. Parameter values are the same as in figure 2. At a given time, the plot shows the values of the 23 'coarse variables'; the first three (S/N_{ref}, I/N_{ref} and R/N_{ref}) are shown in (*a*), while $g_I(x_j)$, $j = 1, \ldots, 10$, and $g_R(x_j)$, $j = 1, \ldots, 10$, are shown in (*b*) and (*c*), respectively. Notice the linear growth of the last 20 modes, showing a uniform drift in strain space. These modes capture the shape of the ICDFs of the I_i and R_i variables, like contour curves. As time progresses, the shapes of the pulses approach an invariant profile so the lines in the two lower graphs become parallel. (*d*) Evolution in time using projective forward integration. The method uses an estimation of the time derivative in the low-dimensional representation, computed after a short run of the stochastic time-stepper; the projective 'jumps' are marked by thin lines.

In addition to the discreteness of the number of the individuals in a population (smoothened through averaging many realizations of the process), our strain space is discrete, and the solutions can then only have discrete translational invariance (shift by a single strain along the lattice). A travelling wave in a spatially discrete problem will then appear in a travelling frame as a (small-amplitude) oscillation: it takes a finite amount of time for the entire shape to progress by exactly one lattice

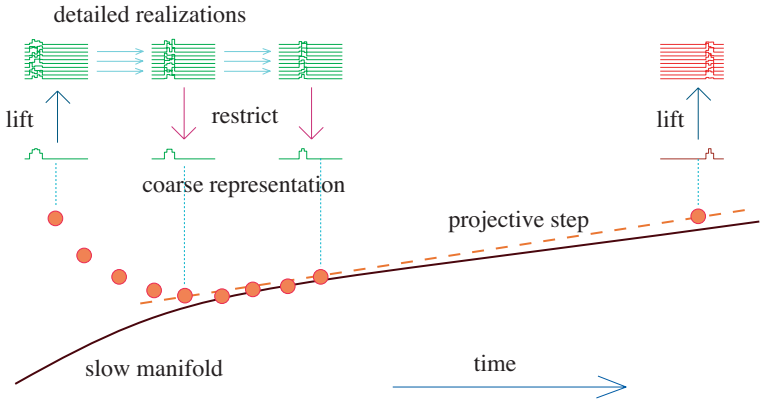

Figure 5. Schematic representation of explicit coarse projective integration. Translation between coarse representations and detailed realizations is implemented through lifting and restriction operators. An initial 'healing' period is required before the detailed simulation approaches the slow manifold and the coarse time derivative is estimated, followed by a projection forward in time. A single (forward Euler) projective step is shown here.

spacing. When this discreteness-induced modulation is relatively small (as is the case here) it is still possible, as we mentioned above (see Moeller *et al.* (2004) for a detailed discussion), to construct a coarse time-stepper for an *effective-continuum* equation. This is accomplished once more by averaging over several, slightly shifted, *discrete space* realizations of a spatially continuous initial shape. It is such *effectively translationally invariant* pulses that we compute here.

The coarse time-stepper takes an initial condition y in the low-dimensional, continuum state representation, 'lifts' to microscopic realizations consistent with it, evolves using the stochastic simulator over time τ based on the individual events such as mutations and infections, and restricts the averaged results onto the same low-dimensional space. This yields a map Φ_τ:

$$y \mapsto \Phi_\tau(y) = \bar{\Phi}_\tau(y) + \xi,$$

where ξ is some noise that persisted even after taking the average over many (here 10–250) realizations. If the system has coarse stationary states, then we should be able to estimate them from the statistics of the map Φ_τ, in particular from a number of pairs $(y, \Phi_\tau(y))$.

A variety of algorithms can be used to find the fixed point z of the coarse time-stepper. In particular, close to this fixed point z, using the Jacobian J of Φ at z we have

$$y_1 = z + J \cdot (y_0 - z) + \xi + o(y_0 - z).$$

If we have many realizations (through Monte Carlo simulation)

$$\{(y_{0,i}, y_{1,i} = \Phi(y_{0,i}))\}_{i=1\ldots N},$$

we can estimate z and J from the minimization of the residual:

$$\sum_{i=1}^{N} \|y_{0,i} - J \cdot y_{1,i} - J \cdot z\|_2^2.$$

Setting $w \stackrel{\text{def}}{=} J \cdot z$, the estimation can be done by solving two linear systems, first for J and w, then for z. Given the noisy nature of the problem, the singular value decomposition is used to invert the relevant matrices in the appropriate subspaces (usually two or at most three dimensional). An estimation of the full Jacobian would require integrations of the system with many different initializations. This method, 'wrapped' as an iterative computational superstructure around the microscopic simulator, may accelerate the convergence to stable stationary solutions, and is capable of converging to such solutions even if they are dynamically *unstable*.

In a more general context, matrix-free methods for solving nonlinear equations (e.g. Newton–Krylov methods using GMRES (Kelley 1995) based on the coarse time-stepper) can be wrapped around the coarse time-stepper to locate stationary solutions of the unavailable coarse equations. The recursive projection method (Shroff & Keller 1993) is one such algorithm that we have extensively used and from which our original inspiration developed. Such algorithms enable a direct simulation code to perform tasks (such as fixed-point computation) that they have not been in principle designed for. It is reasonably straightforward to extend the scope of such a computational *enabling technology* to allow direct simulators to perform continuation, bifurcation and stability analysis, but also controller design and optimization tasks computationally. Upon convergence of the fixed-point algorithms, in particular, matrix-free eigensolvers (subspace iteration methods, Arnoldi methods based on the time-stepper) can be used to extract estimates of the eigenvalues of the linearization of the unavailable population-level equation thus quantifying coarse stability (see discussion in Kevrekidis *et al.* (2003)).

(*c*) *Continuation of coarse solution branches*

We now present two exploratory sets of computations for the dependence of the speed of the effective pulse on two parameters: the strength of infection, quantified by the non-dimensional number R_0 and the (average) number of individuals in the population, N. The (rather low) accuracy shown in both figures can be improved using a larger number of realizations every time the coarse time-stepper is used. This can be accomplished through massively parallel computations, where each processor computes a different realization of the same coarse initial condition for a short time. Here only 250 realizations were used, integrated over a (horizon) time $\tau = 0.5\,\text{yr}$. We used a simple version of continuation: for every new value of the parameter, the predictor of the new stationary state was obtained through linear extrapolation from two previously computed fixed points

$$y^{(0)}(p_{k+1}) = y(p_k) + \frac{(p - p_k)}{(p_k - p_{k-1})}(y(p_k) - y(p_{k-1})),$$

and the corrector in the computation of the fixed point $y^{(\infty)}(p_{k+1}) = y$ was the iterative procedure described above.

We can observe in figure 7*a* how the speed depends on the number R_0, suggesting a relation of the form $c \propto \sqrt{R_0 - 1}$. The existence of a critical value for R_0 can be rationalized using the one-strain model at the fluctuation-free, infinite population limit. If $R_0 \gtrsim 1$, then there is an epidemic equilibrium with $I \ll N$ and very low chances of developing a mutant. But if a single mutant appears, he/she is going to draw the whole population to the new strain. In figure 7*b*, the speed increases

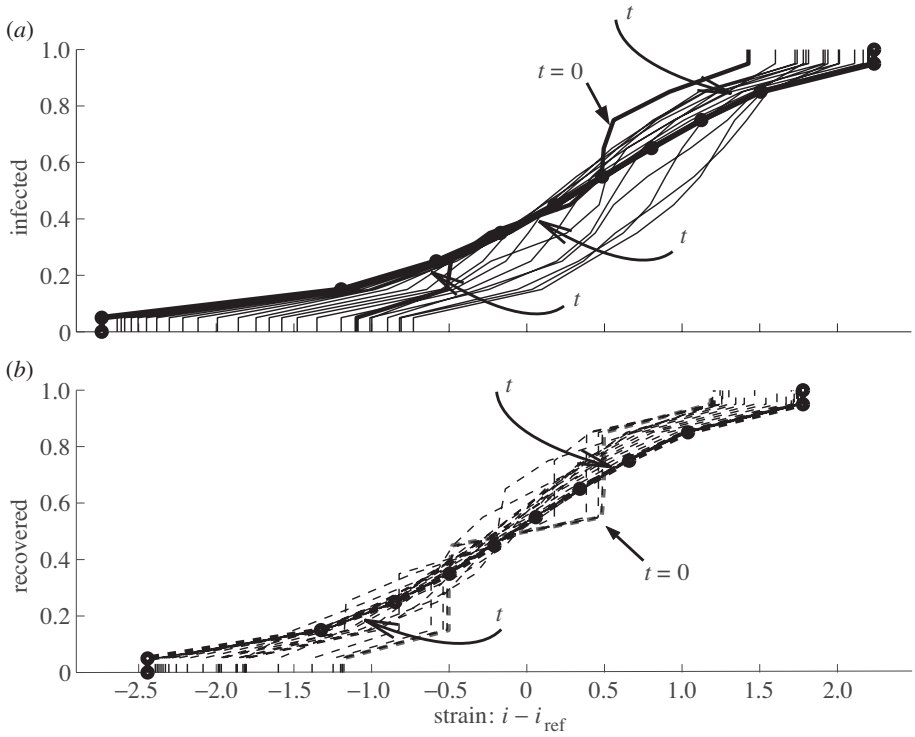

Figure 6. Evolution of the ICDF in the co-evolving frame. Parts (*a*) and (*b*) correspond to the infected and recovered populations, respectively. CDFs at different times are superimposed; the initial distributions are marked. As time progresses, function shapes converge to the thick dashed lines obtained from the fixed points of the coarse representation. Auxiliary arrows show the progression towards convergence. Parameter values as in figure 2.

with the number of individuals, a fact that can also be explained intuitively, as the probability of having an individual mutation (the 'bottleneck') increases with the size of the population. The curve is far away from converging, even for $N \sim 10^8$ individuals. The similarity with $c - c_\infty \propto 1/(\log N)^2$ suggests that some of the ideas of Brunet & Derrida (1997, 1999) may also apply in this epidemiological model: the discreteness of the population affects, in particular, the tails of the distribution where some bins have 0 or 1 individuals.

5. Summary and outlook

We have illustrated the use of equation-free coarse time-stepper-based techniques enabling the macroscopic system-level study of stochastic individual-based evolutionary epidemiology models. The technique circumvents the derivation of macroscopic population-level equations for the expected behaviour of the system; it uses short bursts of appropriately initialized ensembles of individual-based simulation to *estimate on demand* the quantities necessary for system-level analysis. Beyond coarse integration, techniques such as fixed-point algorithms, continuation and bifurcation/stability analysis are thus enabled (on a light note, consider that 'Newton' iteration is performed to find the fixed points of 'Darwinian' evolution models).

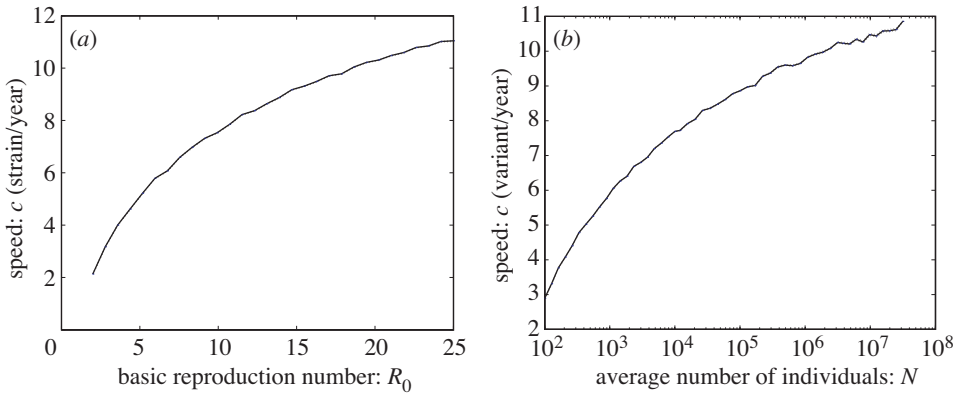

Figure 7. (*a*) Computed speed of the travelling pulses as we change the basic reproduction number R_0. The average number of individuals was 10 000. (*b*) Computed speed of the travelling pulses as we change the (average) number of individuals. We used $R_0 = 10$. Other parameters as in figure 2.

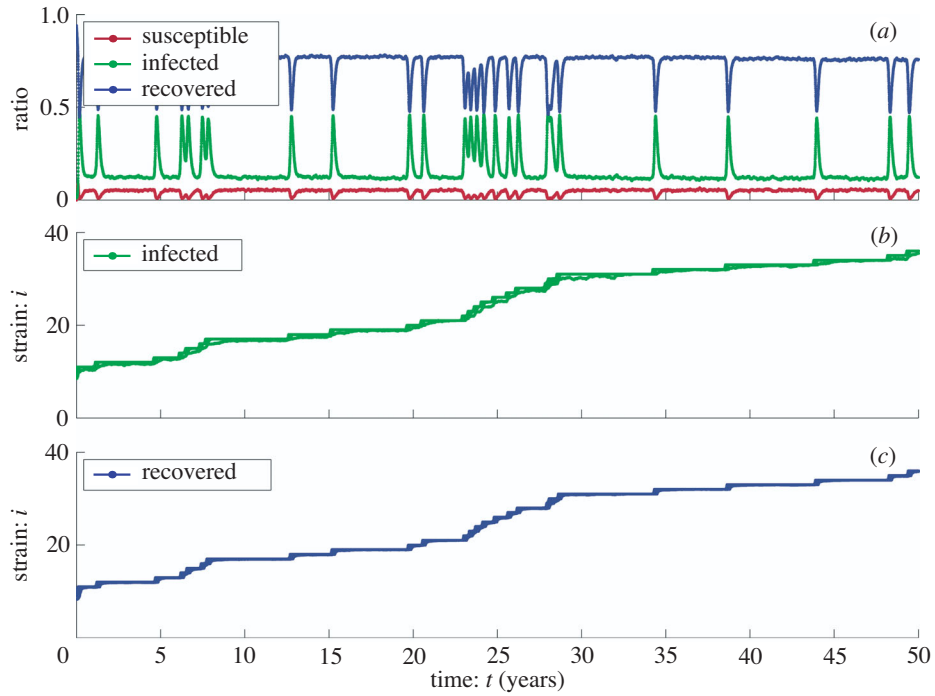

Figure 8. Time evolution for a low value of the mutation rate $p = 0.000\,12\ \mathrm{yr}^{-1}$. Other parameters as in figure 2. (*a*) Ratios S/N, I/N and R/N. The number of infected and susceptible individuals are close to zero most of the time, except right after a new mutation arises. (*b*), (*c*) Approximations of the ICDFs for the infected and the recovered populations, respectively. Travelling pulses become very narrow (one circulating strain), and long quiescent periods are punctuated by sudden jumps that follow the mutation of a single individual that rapidly infects the rest of the population with the new strain, followed by fast recruitment and recovery.

The approach holds promise in studying emergent behaviour in individual-based or agent-based models across several disciplines. Parametric analysis can be performed directly in terms of microscopic interaction parameters as well as of parameters such as the population size. Various extensions of the approach that have been discussed in other contexts (see, for example, Kevrekidis *et al.* 2003) can also be brought to bear in epidemiological modelling: the so-called *gap-tooth scheme* and *patch dynamics* have the potential to accelerate simulations of quantities smoothly distributed over several variables. Techniques based on matrix-free iterative eigenanalysis can also be used to explore when (in parameter space) and how a closure fails, and to establish whether alternative coarse descriptions of the system (e.g. with more coarse variables) may be useful.

Finally, we believe the combination of such coarse techniques with optimization and the approximation of effective free energy surfaces may prove useful for the quantitative study of extinction probabilities and epidemic thresholds; the simulation in figure 8 is suggestive of the 'rare event' nature of the epidemic propagation under such conditions. For small values of the mutation rate the pulse itself becomes very narrow, and the number of infected individuals very small, as most of the individuals become recovered. Drift occurs only if one infected person mutates to the right $\mathcal{I}_i \mapsto \mathcal{I}_{i+1}$ and infects the population of immune individuals to strain i with the new strain $i+1$, producing a shift of one strain to the right. The speed of these 'punctuated pulses' appears proportional to pNi^*, the mutation rate times the number of individuals in the infected class at equilibrium.

Several aspects of equation-free modelling are applicable in mathematical epidemiology. This paper is intended as a proof of principle, outlining the computational methodology and demonstrating the emergence of pulses—more generally, evolutionary patterns—in sequence evolution. We are currently using this framework to investigate the important case of the evolution of the influenza A virus, restricting the SIRS model to forbid loss of immunity; we intend to extend the approach to a much broader class of applications.

We are grateful for valuable discussions with Juan Lin, Viggo Andreasen, Jonathan Dushoff and Gerhard Hummer. This work was partly supported by the AFOSR, and a NSF-ITR grant. S.A.L. gratefully acknowledges the support of the National Institutes of Health, award no. 1-R01-GM60729-01.

References

Andreasen, V., Levin, S. & Lin, J. 1996 A model of influenza A drift evolution. *Z. Angew. Math. Mech.* **76**(2), 421–424.

Brunet, E. & Derrida, B. 1997 Shift in the velocity of a front due to a cutoff. *Phys. Rev.* E **56**(3), 2597–2604.

Brunet, E. & Derrida, B. 1999 Microscopic models of traveling wave equations. *Comput. Phys. Commun.* **121–122**, 376–381.

Carter, E., Ciccotti, G., Hynes, J. & Kapral, R. 1989 Constrained reaction coordinate dynamics for the simulation of rare events. *Chem. Phys. Lett.* **156**(5), 472–477.

Chen, L.-Y. & Goldenfeld, N. 1995 Numerical renormalization-group calculations for similarity solutions and traveling waves. *Phys. Rev.* E **51**, 5577–5581.

Chorin, A., Kast, A. & Kupferman, R. 1998 Optimal prediction of underresolved dynamics. *Proc. Natl Acad. Sci. USA* **95**, 4094–4098.

Chorin, A., Hald, O. & Kupferman, R. 2000 Optimal prediction and the Mori–Zwanzig representation of irreversible processes. *Proc. Natl Acad. Sci. USA* **97**, 2968–2973.

Doering, C., Hagan, P. & Rosenau, P. 1987 Random-walk in a quasi-continuum. *Phys. Rev.* A **36**, 985–988.

Earn, D., Dushoff, J. & Levin, S. 2002 Ecology and evolution of the flu. *Trends Ecol. Evol.* **7**, 355–369.

Fitch, W., Bush, R., Bender, C., Subbarao, K. & Cox, N. 2000 Predicting the evolution of human influenza A. *J. Hered.* **91**(3), 183–185.

Gear, C. 2001 Projective integration methods for distributions. Technical Report NEC TR 2001-1 30, NEC, NJ, USA.

Gear, C. & Kevrekidis, I. 2003 Projective methods for stiff differential equations: problems with gaps in their eigenvalue spectrum. *SIAM J. Sci. Comput.* **24**(4), 1091–1106.

Gear, C., Kevrekidis, I. & Theodoropoulos, C. 2002 'Coarse' integration/bifurcation analysis via microscopic simulators: micro-Galerkin methods. *Computers Chem. Engng* **26**, 941–963.

Hummer, G. & Kevrekidis, I. G. 2003 Coarse molecular dynamics of a peptide fragment: free energy, kinetics, and long-time dynamic computations. *J. Chem. Phys.* **118**(23), 10 762–10 773.

Kelley, C. T. 1995 *Iterative methods for linear and nonlinear equations*. Frontiers in Applied Mathematics, vol. 16. Philadelphia, PA: SIAM Publications.

Kessler, D., Levine, H., Ridgway, D. & Tsimring, L. 1997 Evolution on a smooth landscape. *J. Statist. Phys.* **87**, 519–544.

Kevrekidis, I., Gear, C., Hyman, J., Kevrekidis, P., Runborg, O. & Theodoropoulos, C. 2003 Equation-free multiscale computation: enabling microscopic simulators to perform system-level tasks. *Commun. Math. Sci.* **1**(4), 715–762. (See http://arxiv.org/abs/physics/0209043 for an extended original version.)

Kevrekidis, P., Kevrekidis, I., Bishop, A. & Titi, E. 2002 A continuum approach to discreteness. *Phys. Rev.* E **65**, 046613.

Lin, J., Andreasen, V., Casagrandi, R. & Levin, S. 2003 Traveling waves in a model of influenza A drift. *J. Theor. Biol.* **222**(4), 437–445.

Melchior, M. & Oettinger, H. 1995 Variance reduced simulations of stochastic differential equations. *J. Chem. Phys.* **103**, 9506–9509.

Moeller, J., Runborg, O., Kevrekidis, P., Lust, K. & Kevrekidis, I. 2004 Effective equations for discrete systems: a time stepper based approach. *Int. J. Bifurcation Chaos* (In the press.)

Nåsell, I. 1999 On the time to extinction in recurrent epidemics. *J. R. Statist. Soc.* B **61**(2), 309–330.

Nåsell, I. 2002 Stochastic models of some endemic infections. *Math. Biosci.* **179**, 1–19.

Pease, C. 1987 An evolutionary epidemiological mechanism, with applications to type A influenza. *Theor. Population Biol.* **31**, 422–452.

Press, W., Teukolsky, S., Vetterling, W. & Flannery, B. 1992 *Numerical recipes in C: the art of scientific computing*, 2nd edn. Cambridge University Press.

Ridgway, D., Levine, H. & Kessler, D. 1998 Evolution on a smooth landscape: the role of bias. *J. Statist. Phys.* **90**, 191–210.

Rosenau, P. 1986 Dynamics of nonlinear mass-spring chains near continuum limit. *Phys. Lett.* A **118**, 222–227.

Rosenau, P. 1987 Dynamics of dense lattices. *Phys. Rev.* B **36**, 5868–5876.

Rosenau, P. 1989 Extending hydrodynamics via the regularization of the Chapman–Enskog expansion. *Phys. Rev.* A **40**, 7193–7196.

Rosenau, P. 1992 Tempered diffusion: a transport process with propagating fronts and inertial delay. *Phys. Rev.* A **46**, R7371–7374.

Rowley, C. & Marsden, J. 2000 Reconstruction equations and the Karhunen-Loève expansion for systems with symmetry. *Physica* D **142**, 1–19.

Rowley, C., Kevrekidis, I., Marsden, J. & Lust, K. 2003 Reduction and reconstruction for self-similar dynamical systems. *Nonlinearity* **16**, 1257–1275.

Runborg, O., Theodoropoulos, C. & Kevrekidis, I. 2002 Effective bifurcation analysis: a time-stepper based approach. *Nonlinearity* **15**, 491–511.

Ryckaert, J., Ciccotti, G. & Berendsen, H. 1977 Numerical integration of Cartesian equations of motion of a system with constraints: molecular dynamics of n-alkanes. *J. Comput. Phys.* **23**, 327–341.

Schoenmakers, J., Heemink, A., Ponnambalam, K. & Kloeden, P. 2002 Variance reduction for Monte Carlo simulation of stochastic environmental models. *Appl. Math. Modelling* **26**, 785–795.

Shenoy, V., Miller, R., Tadmor, E., Rodney, D., Phillips, R. & Ortiz, M. 1999 An adaptive finite element approach to atomic-scale mechanics—the quasicontinuum method. *J. Mech. Phys. Solids* **47**, 611–642.

Shroff, G. & Keller, H. 1993 Stabilization of unstable procedures: the recursive projection method. *SIAM J. Numer. Analysis* **30**(4), 1099–1120.

Theodoropoulos, K., Qian, Y.-H. & Kevrekidis, I. 2000 'Coarse' stability and bifurcation analysis using timesteppers: a reaction diffusion example. *Proc. Natl Acad. Sci. USA* **97**(18), 9840–9843.